applied sciences

MDPI

Article

Shake Table Testing of Standard Cold-Formed Steel Storage Rack

Ahmad Firouzianhaij [1], Nima Usefi [1,*], Bijan Samali [1] and Peyman Mehrabi [2]

[1] Centre for Infrastructure Engineering, Western Sydney University, Sydney, NSW 2747, Australia; A.Firouzianhaji@westernsydney.edu.au (A.F.); B.Samali@westernsydney.edu.au (B.S.)
[2] Department of Civil Engineering, K.N. Toosi University of Technology, Tehran 15875-4416, Iran; p.mehrabi@email.kntu.ac.ir
* Correspondence: n.usefi@westernsydney.edu.au

Abstract: Full-scale shake table investigations are strongly required to understand the actual performance of storage racks and to improve the rack design guidelines. This paper presents the results of full-scale shake table tests on New Zealand standard storage rack frames with two-bay and two-level to determine the dynamic characteristics of a standard rack structure and to measure the damping of the system. The experimental program was conducted in three phases. First, the identification parameters including the natural frequency and damping of the system were determined through a series of preliminary tests. Then, shake table tests were performed to capture the inelastic response of rack frames under low to medium intensities of El-Centro ground motion. Finally, the shake-table tests were repeated with scaling down the time domain and broader ranges of ground motion intensities to consider the performance of taller rack systems. In addition, a comprehensive discussion on the damping of the system is also provided based on the test results. The performance of the rack frame is described through an extensive set of measurements, including rack displacement, pallet sliding, the acceleration of a concrete block and rack frame and the damping of the system in the down-aisle direction. The results indicate that the standard rack frames are able to endure large inelastic deformations without loss of stability.

Keywords: storage rack; cold-formed steel; shake table; damping; ground motion; earthquake; frequency; pallet

Citation: Firouzianhaji,A.; Usefi, N.; Samali, B.; Mehrabi, P., Shake Table Testing of Standard Cold-formed Steel Storage Rack. *Appl. Sci.* **2021**, *11*, 1821. https://doi.org/10.3390/app11041821

Academic Editor: Amadeo Benavent-Climent
Received: 19 January 2021
Accepted: 14 February 2021
Published: 18 February 2021

Publisher's Note: MDPI stays neutral with regard to jurisdictional claims in published maps and institutional affiliations.

Copyright: © 2021 by the authors. Licensee MDPI, Basel, Switzerland. This article is an open access article distributed under the terms and conditions of the Creative Commons Attribution (CC BY) license (http://creativecommons.org/licenses/by/4.0/).

1. Introduction

Being part of the Pacific Ring of Fire, which is geologically active, New Zealand has experienced many large earthquakes in the past decades. One of the recent large earthquakes was the 2010 Canterbury earthquake (also known as the Christchurch earthquake or Darfield earthquake) that rocked the south island of New Zealand with a magnitude of 7.1 on the Richter scale. Figure 1 illustrates the various rack failure mechanisms observed and recorded after this earthquake. Some of the frames collapsed (Figure 1a) when a plastic hinge was formed in the uprights, which resulted in further drift and the amplification of second-order effects and thereby caused the failure of the system. It was also observed that, despite the basic assumptions for seismic design and stability analysis, "linear deformation of the frame" is not an accurate assumption and therefore not all the connections experience the same rotation along the frame height (Figure 1b). The use of an insufficient number of bolts in typical baseplate connections also led to excessive rotation and failure of the base plate, as shown in Figure 1c. The cyclic deterioration of such connections also triggered a progressive collapse of all frames in the warehouse [1–5] (Figure 1d), which indicates that the current racking codes and specifications are still weak about the cyclic features of the connections.

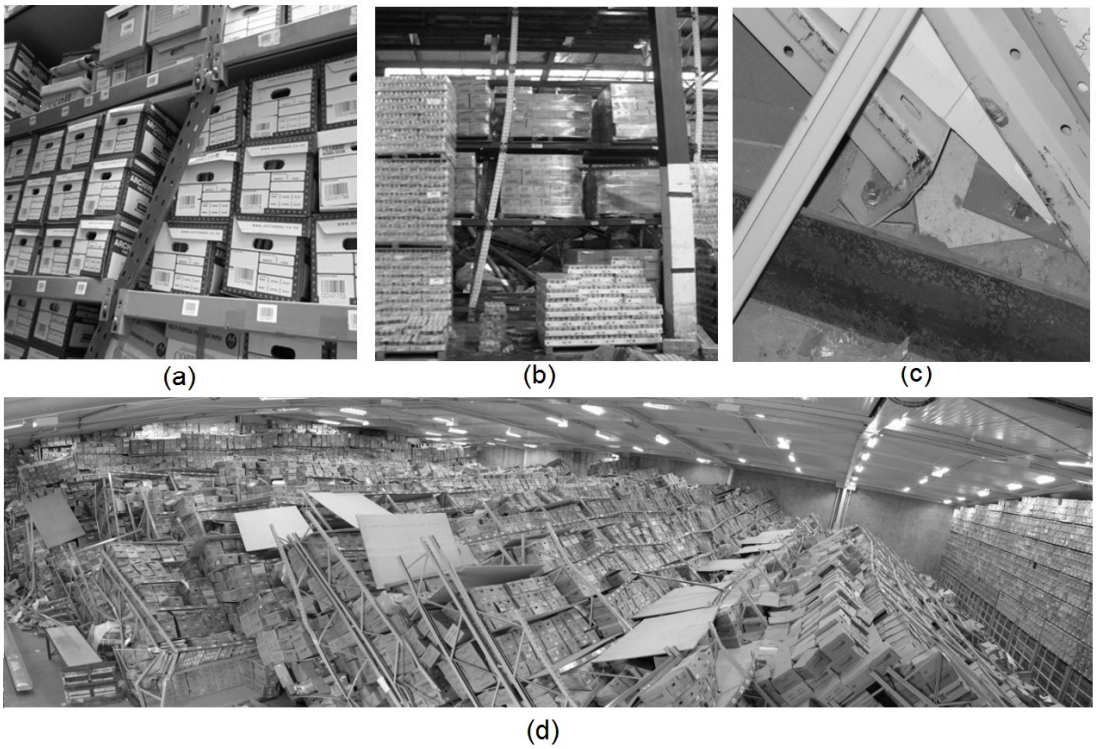

Figure 1. Different rack failure mechanisms during the Christchurch earthquake: (**a**) down-aisle mechanism, (**b**) down-aisle mechanism, (**c**) baseplate deterioration in cross-aisle direction, (**d**) progressive collapse of the entire system.

Storage rack structures are mainly designed for seismic actions based on rack provisions, including the Rack Manufacturers Institute (RMI) specification [6], European code (EN 16681) [7], Australian standard (AS 4084) [8], Federal Emergency Management Agency (FEMA 460) [9], Canadian Standards Association (CSA A344) [10] and American National Standards Institute (ANSI MH16) [11]. Nevertheless, in many regions, the design of racking frames is still based on general seismic design codes due to the lack of enough guidelines for the dynamic design of rack frames. Additionally, some of the current seismic design standards allow the use of the equivalent static method to estimate the seismic forces and do not consider the sliding of the frame (or only consider the rocking of pallets on the rack beams) for the design procedure. It should be noted that a significant contribution to the seismic response of rack frames can be rocking [12,13]. Therefore, to examine whether the principals provided in the codes are adequate and sufficiently accurate for rack systems, it is worth investigating their performance under severe seismic ground motions.

Although static and cyclic tests and analyses can reveal the failure mode of rack components [14–20] and the associated base shear of a rack structure, a more realistic structural response (such as acceleration) can be attained through full-scaled shake table tests [21]. One of the first shake-table studies on storage racks was conducted by Chen et al. [22–24] who tested four types of full-scale industrial steel storage racks under scaled ground motions of El-Centro (ELC) and Parkfield earthquakes. The shake table tests demonstrated that the P-delta effects meaningfully influence the response of the racks in the down-aisle direction. In another shake-table study, Filiatrault et al. [25] tested five different rack frames in both cross-aisle and down-aisle directions and reported that the ductility and energy dissipation capacity of the frame were significantly more in the down-aisle direction than in the cross-aisle direction. A comprehensive shake table program was carried out at the University of Buffalo on four steel storage rack configurations, and it was stated that the rotational stiffness of beam-to-upright connections was significantly

affecting the down-aisle performance of pallet racks under seismic actions [26]. In another attempt, Filiatrault et al. [27] characterized the seismic performance of the rack frames under earthquake excitation and identified the pallet shedding fragility under a series of ground motions through shake table testing. In addition to the classical design of rack frames against seismic loads, the isolation systems, such as fuse elements, can also be adopted for a rack frame, which brings benefits in terms of a reduction in the structural damage and improving the safety of the stored items [28–33].

Shake table tests performed by Rosin et al [34] also revealed that the eccentric bracing configurations could lead to a significant torsional response. Gilbert and Rasmussen [35] evaluated a complete drive-in rack system under loaded and empty conditions using a full-scale shake table, and provided the relative stiffness under different ground motion conditions. Recently, new shaking table tests were conducted on storage racks in the cross-aisle direction in order to obtain the seismic characteristics of the system in this direction [36,37].

Considering the current increasing demand on rack storage systems as well as the improvements of storage rack regulations, the need for understanding the dynamic response and seismic characteristics of the standard rack frames, i.e., damping of the system, under actual strong ground motions has been intensified. Therefore, the objective of this paper is to provide the results of shake table tests on a New Zealand standard rack frame with two bays and two levels under increasing seismic base excitation in the down-aisle direction, aiming to reveal the dynamic features of a standard steel storage rack under actual seismic actions. The experimental program was conducted in three stages. In the first stage, identification tests were carried out to determine the fundamental period of vibration and the damping ratio of the system. In the second stage, the frame was tested by 20–80% intensities of El-Centro earthquakes in an actual time domain. In the third stage, the tests were repeated with a wide range of intensities, 40–220% of El-Centro earthquakes, with scaled records in the time domain to consider the performance of taller rack systems. The damping of the system is also determined and the results are presented for both the scaled and non-scaled time-domain conditions. The test results of this study can be valuable data for the calibration of finite element models as well as seismic provisions for the design of racks.

2. Experimental Program

2.1. Rack Geometries

To evaluate the seismic performance of the storage rack systems in the down-aisle direction, fifteen full-scale shake table tests were conducted at different stages. The configuration and geometry of the specimens were defined based on New Zealand standard storage rack pallets to simulate the behaviour of actual pallets used in seismic areas.

The racks were of conventional two-bay and two-level rack frames, as shown in Figure 2. The width of each bay in the down-aisle and cross-aisle was 1440 mm and 900 mm, respectively. The height of each level was 1275 mm. All rack specimens were built from typical cold-formed steel (CFS) sections with G350 grade steel. Bracing elements were of C channel profiles with 25 mm depth, 30 mm flange and 1.8 mm thickness and were installed in the cross-aisle direction with 600 mm pitches. The upright profiles of 90 mm depth and 2.5 mm thickness were connected in the down-aisle direction by 1.6 mm thick 105 × 50 mm box beams. The geometry of the section as well as the perforation details are indicated in Figure 3. Due to commercial confidentiality reasons, all geometries are presented in non-dimensional form—the same as other studies in this area [38]. Table 1 tabulates the cross-sectional properties of the structural elements used in the rack specimens. The beam to upright connections were of boltless type (hooked connectors), which are commonly utilized in most rack systems due to the easier and faster installation of frames. The frames were anchored to a 30 mm thick steel plate, which was placed on

the shake table using bolted connections. Two types of baseplates were used in the tests, for the side and middle spans, as shown in Figure 4. To simulate the actual condition of palletized merchandise, each pallet was accommodated with two standard precast concrete blocks. Each concrete block weighed approximately 500 kg with dimensions of 755 mm × 565 mm × 510 mm, which is a normal value for the merchandise used in practice. Therefore, each specimen could contain eight concrete blocks over its two beam levels, which provided a 4000 kg pallet load in total and simulated a fully-loaded service condition. The rack specimen and the concrete blocks are shown in Figure 5.

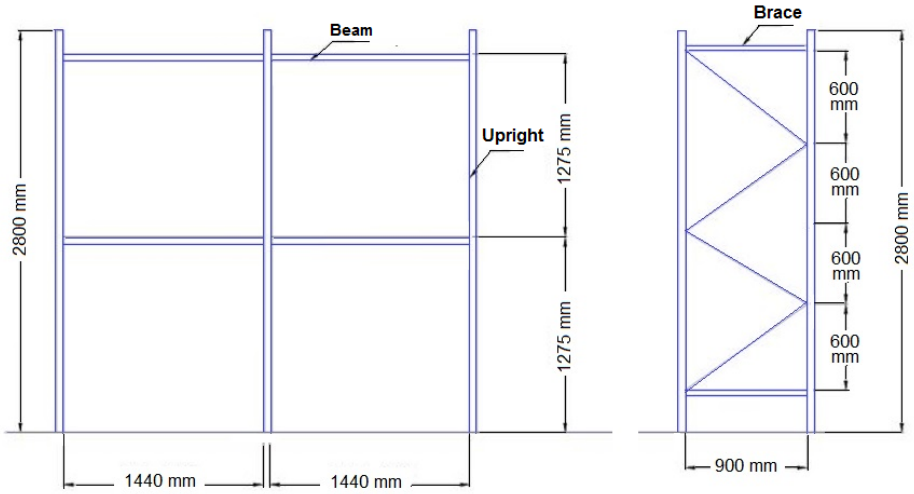

Figure 2. Schematic views and dimensions of the frame.

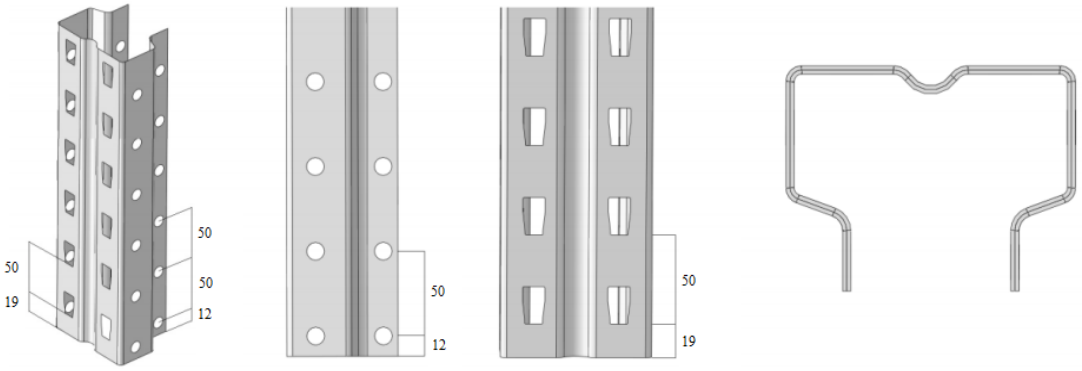

Figure 3. Section and perforation details.

Table 1. Section details.

Element	Section	Length (mm)	Area (mm²)	Ix (mm⁴)	Iy(mm⁴)
Beam	Box105 × 50-1.6 mm	1350	597	1,023,099	237,210
Upright	90 Upright 2.35 mm	2800	578.6	700,217	325,825
Brace	25 × 30 × 1.8 (C Channel)	1062	217	19,956	11,388

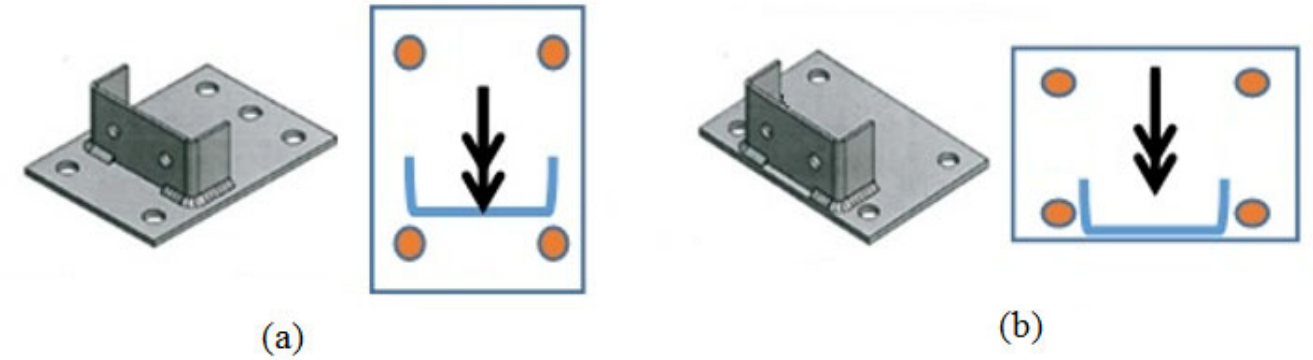

Figure 4. Different baseplate connections: (**a**) middle frame, (**b**) side frame

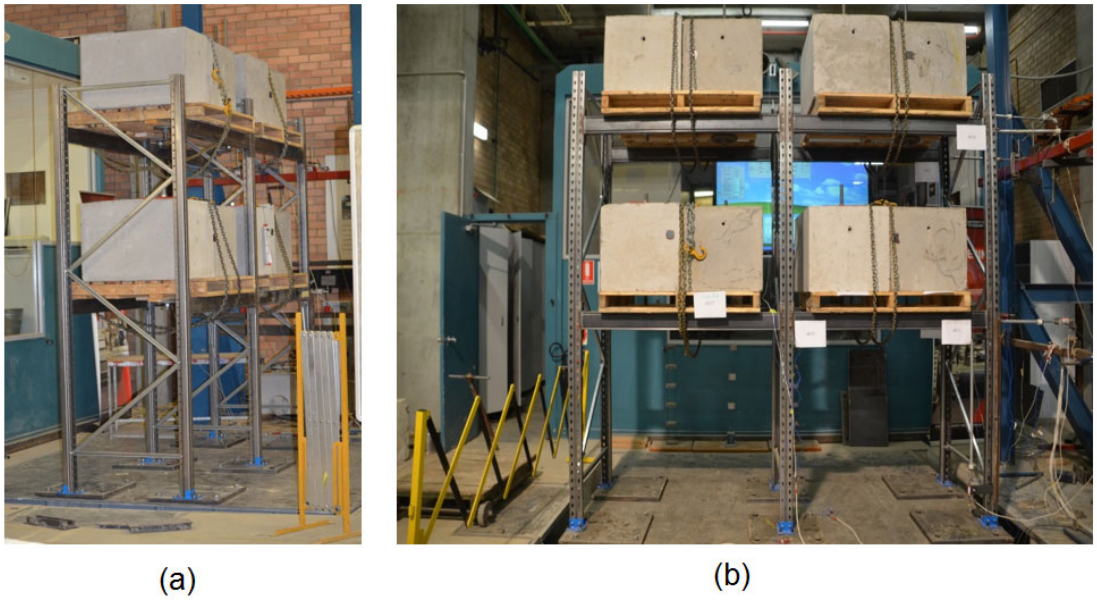

Figure 5. Rack frame with block weights: (**a**) cross-aisle direction, (**b**) down-aisle direction.

2.2. Test Setup and Instrumentation

All tests were performed on a 3 m × 3 m uniaxial shake table at the University of Technology, Sydney. The shake table used for the tests is a uni-directional table and is digitally programmable with feedback control to simultaneously control displacement, velocity, and acceleration.

The shake table had a payload capacity of 10 tonnes and an overturning moment capacity of 10-tonne meter.

Two different types of instrumentation, including accelerometers and displacement transducers, were employed for recording the response of rack frames. Six accelerometers were attached to the frame (three for the rear and three for the front of the rack) and the other two were installed to the concrete blocks. In addition, four Linear Variable Differential Transformer (LVDT)s were employed to record the displacements of the rack frames, and one LVDT was used to measure the displacement of a typical pallet during the tests. The LVDTs and accelerometers were attached to both sides of the frames (front and rear) to identify the probable rotation of the rack in each level. The shaking table actuator was also equipped with an LVDT and an accelerometer to record the table displacement and the ground acceleration in the direction of motion. The location of the instrumentations is illustrated in Figure 6. A typical accelerometer and LVDT connected to the frame and concrete block are also shown in Figure 7.

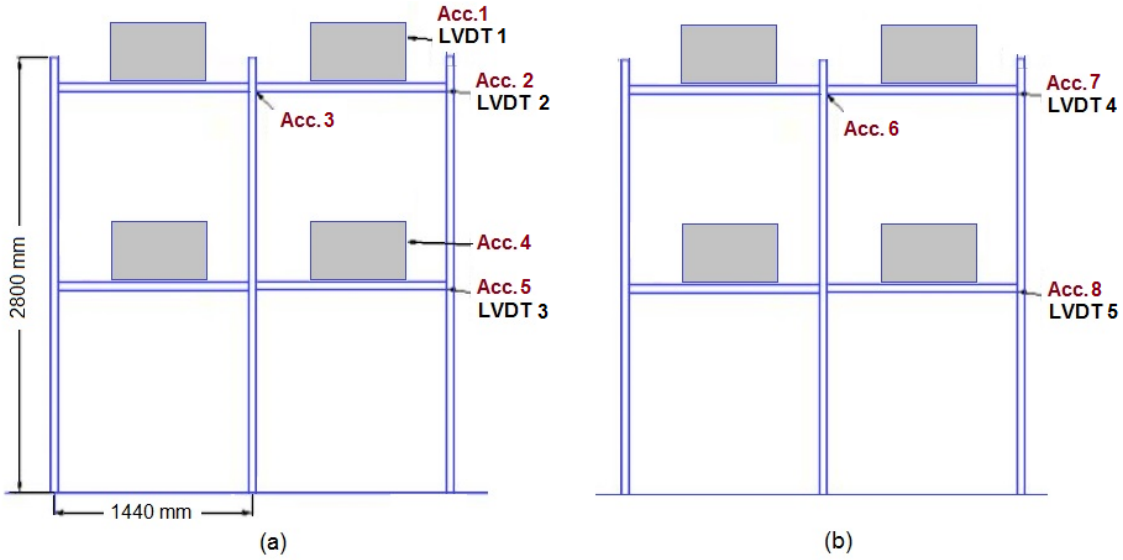

Figure 6. Location of Linear Variable Differential Transformers (LVDTs) and accelerometers: (**a**) front frame, (**b**) back frame.

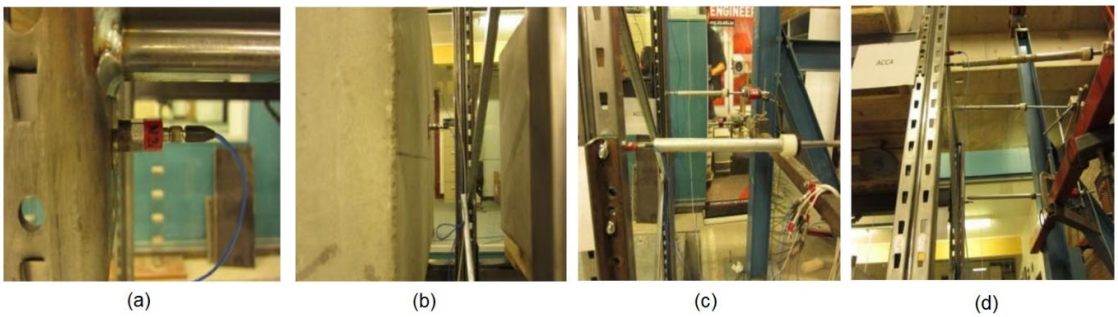

Figure 7. Instrumentations: (**a**,**b**) accelerometer attached to frame and concrete block, (**c**,**d**) LVDT attached to frame and concrete block.

The concrete blocks were fixed to the timber pallets by means of steel rods and bearing plates to prevent them from sliding on the pallets. The pallets were also chained to the beam to avoid them falling off the frame, as shown in Figure 5. To minimize the catastrophic collapse of the rack subjected to higher seismic records, support structures were also designed and constructed to allow the structure to lean against in case of failure. Figure 8 displays the rack frame and supporting structure.

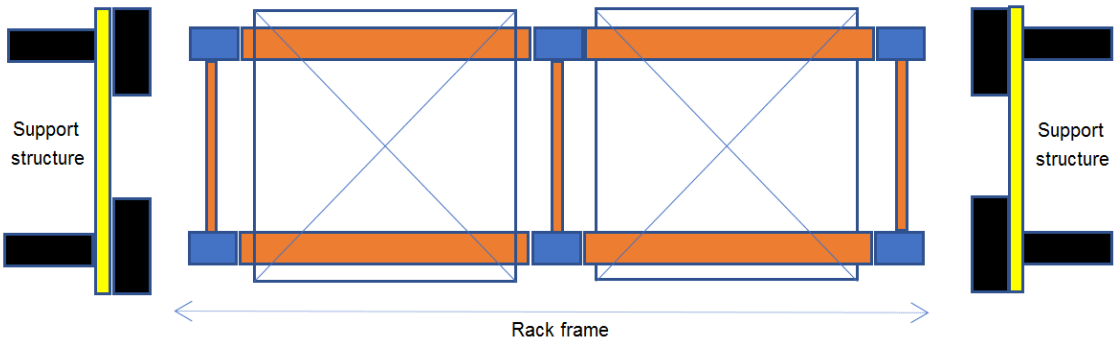

Figure 8. Schematic plan view of rack frame and support structures.

2.3. Testing Protocol

The experimental tests on the rack specimens were performed in three phases. Phase one of the experimental test was conducted to determine the dynamic characteristics of the rack system, including the natural frequency and damping coefficient of the rack, which are named as system identification tests. Phase two and three of the experiment were undertaken to evaluate the seismic response of the rack frames through the actual shake table tests under non-scale and scaled time-domain conditions, respectively. Table 2 shows the details of each experimental phase.

Table 2. Summary of the experimental tests.

Test Phase	Time Scaling Factor *	Earthquake Record	Intensities (%)
One	1	Northridge (1994)	10
		El-Centro (1940)	20
Two			20, 40, 60, 70, 80
Three	2		40, 60, 80, 100, 120, 140, 160, 180, 200, 220

* The earthquake record's scaling factor in the time domain.

2.3.1. Phase One: System Identification Tests

Identification of frequency and natural period: The identification phase requires the adoption of a suitable identification algorithm [39,40]. In this study, Sine sweep tests were performed to identify the natural period of the rack system in its original condition—same as other studies on CFS rack frames [41].

Therefore, a full-cycle acceleration time-history at frequency ranges of 0.5 to 20 Hz with a rate of one octave per minute and an amplitude of 0.025 g was generated by the shake table in the down-aisle direction of the rack. LVDTs and accelerometers were also used for the identification test.

Identification of damping: Damping is an essential factor in the seismic field. A hammer test and a hand exciting test were conducted to measure the preliminary damping coefficient of the system before performing the shake table tests. In the former method, different parts of the rack were excited by hammer impact, while in the latter approach, the rack was shaken for three cycles and then was left to have free vibration. It should be noted that the damping ratio was also determined by the sine sweep test after each shake table test, to compare the damping ratio before and after motion.

2.3.2. Phase Two and Three: Shake Table Tests

The objective of these two phases was to capture the seismic response of the standard rack system under various intensity ground motions and different time-domain scales. The excitation intensity was therefore applied in an incremental fashion. The loading schedule in phase two and phase three of the experiment was as follows:

- In phase two, the tests started at a Peak Ground Acceleration (PGA) of 20% of the 1940 El-Centro earthquake record, and then the earthquake record was increased by steps of 10% or 20% (increasing 10–20% of the PGA for shake table excitation in each step) up to 80% intensity of the El-Centro earthquake. The shake table tests were conducted without scaling time domain.
- In phase three, the shake table testing program was carried out to subject the rack frame under a range of intensities between 40% and 220% of the El-Centro earthquake record. The increment increase was continued until a significant drop in the fundamental period of the system was observed, which indicates the formation of local plastic deformation in the structure. In this phase, the time domain was scaled down by a factor of 2 to better simulate the sensitivity of taller racks with elongated periods.

As stated earlier, sine sweep tests with a low intensity (0.02 g) were also conducted after every seismic excitation (each increment) to evaluate the damping ratio as well as monitoring possible period elongation due to damage in the system.

3. Test Results

3.1. Results of Phase One: System Identification Tests

The preliminary test schedule of phase 1 was only conducted to provide an indicative understanding of the rack natural behaviour under dynamic actions. Sine sweep test results presented in Figure 9a are in the form of Fast Fourier transform (FFT) to easily determine the frequencies of vibration (using a pre-programmed laboratory software). The sine sweep results indicate that the fundamental frequency of vibration is around 1.6 Hz, which corresponds to the vibration period of 0.63 seconds. Mode shapes were similar to those reported by Krawinkler [42]. The first and second modes of vibration were quite visible; however, the third mode was not visible to the naked eye. Figure 9b schematically shows the first and second modes of vibrations.

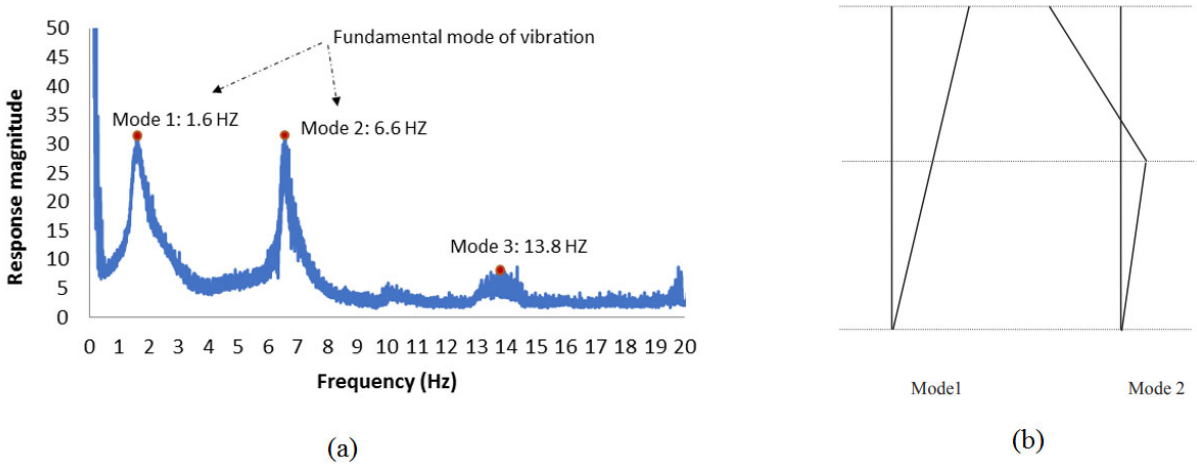

Figure 9. (**a**) Fast Fourier transform (FFT) of sine sweep test of the specimen before being exposed to any seismic actions, (**b**) first and second modes of vibration observed in sine sweep test.

The damping coefficient was also obtained from the decay of the free vibration response from the handshake test and the hammer test, as shown in Figure 10. The damping of around 9% was captured from these tests. It is notable that damping values could be higher if more practical pallet weights had been used in lieu of rigid concrete blocks. In addition, the weight of the pallets would also influence the damping values.

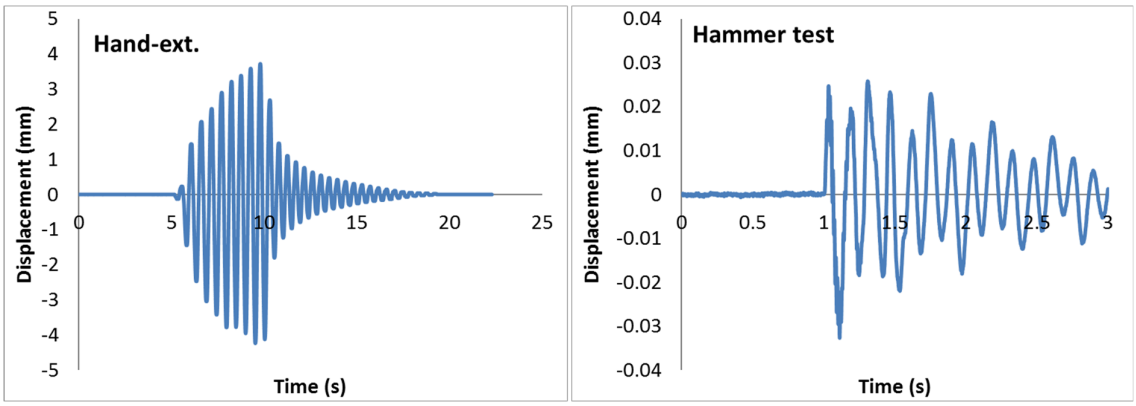

Figure 10. Hand exciting and hammer test to measure damping.

Precaution needed to be taken to ensure safety and avoid the global instability of the rack specimen during shake table tests. Therefore, prior to conducting the shake table tests, preliminary numerical models of the rack specimens were developed in order to find the critical parameters of "overall overturning moment" and "top-level displacement" and to check them against the maximum allowable values of the shaking table device. The numerical model was verified using the frequency and damping coefficient obtained in phase 1 of the experiment.

3.2. Results of Phase Two: Shake Table Tests (Non-Scaled in The Time Domain)

Figure 11 shows the structural responses under 20% to 80% intensity of the El-Centro earthquake record without scaling the time domain in terms of accelerations in the top and bottom levels and the lateral displacement of the rack frame. The experimental data of the back frame are only shown in this figure since the results of the front and back frame were almost identical, indicating that no rotation occurred during the tests. It was decided not to subject the specimen to a record greater than 80% of the El-Centro earthquake as the recorded acceleration of the top-level indicated a peak acceleration near "1.0 g", which was close to the capacity of the shake table under a 4-tonne structure. As shown in Figure 12, pallet sliding occurred in all specimens; however, no significant pallet movement was observed during the tests with intensities of 20% and 40%. Sliding was much more pronounced for intensities of 70% and 80%, with maximum sliding of around 27 mm and 18 mm in the top pallet, respectively. For this reason, the top pallet acceleration (Effective Design Acceleration (EDA) started to deviate from the acceleration that was recorded from the accelerometer mounted to the upright, as shown in Figure 12.

Measured peak responses of the rack structure under seismic actions are tabulated in Table 3. A comparison between first and second level accelerations and displacements as well as the base shear of the rack system is also provided in Figure 13. The deformation of the structure under seismic actions indicates that the inter-storey drift of the first level is significantly higher than the second level inter-storey drift. This trend becomes more obvious by increasing the seismic intensity, which was indicative of a soft storey failure mode of the structure [43–45]. The base shear shown in Figure 13 is also calculated from the two accelerometers placed on the pallets at two levels times the mass of the pallets (rack mass is negligible). The base shear results demonstrate that the rate of increasing base shear is lower at higher intensities, though the base shear is generally enhanced by increasing the earthquake intensities. The difference between pallet and rack accelerations, presented in Table 3, is mainly due to the sliding of the pallet on the frame where this difference is more significant at higher intensities (owing to greater sliding of the pallet).

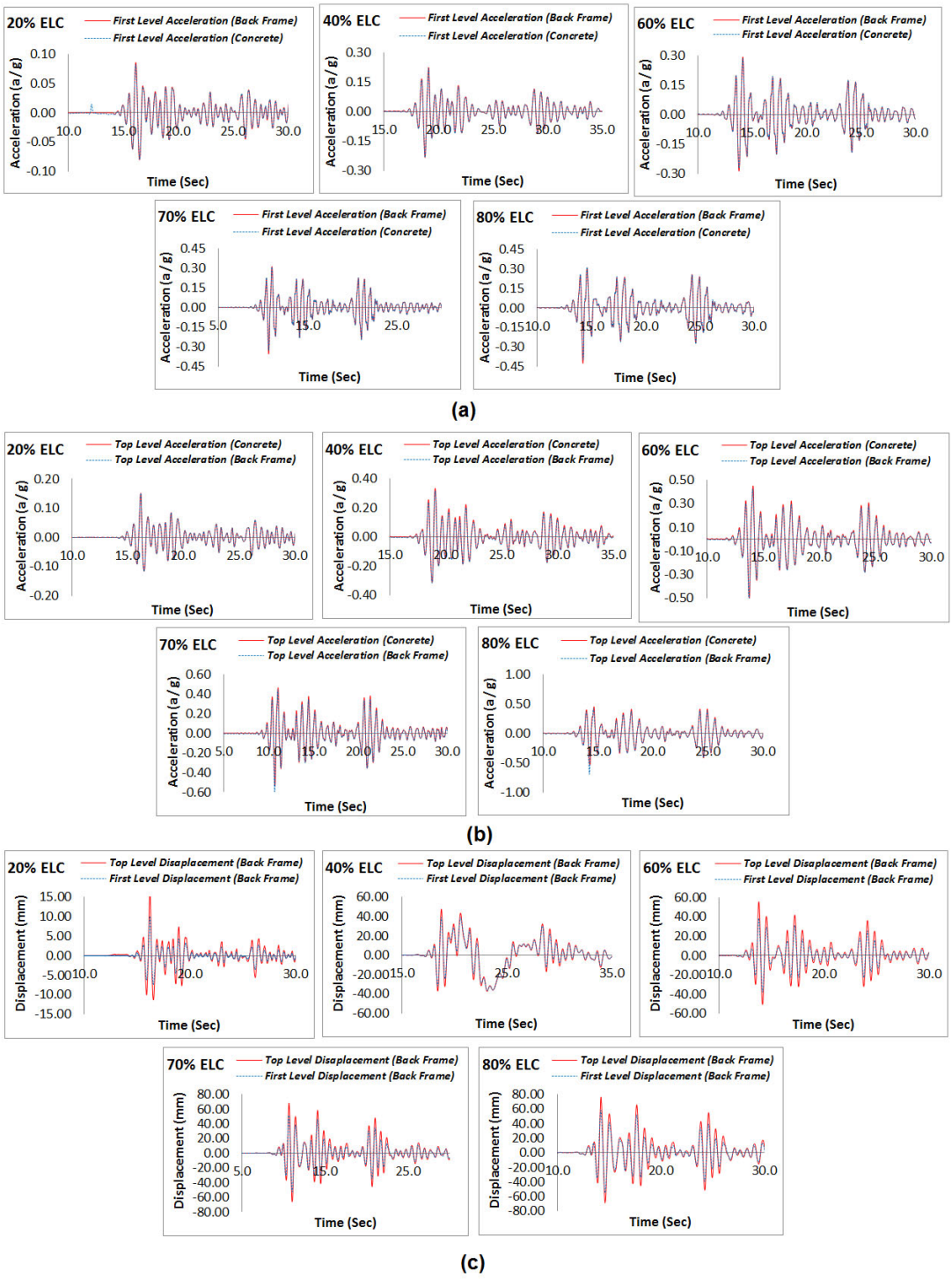

Figure 11. Structural response under 20–80% intensity of El-Centro (ELC) earthquake record—Non-Scaled in time domain: (**a**) accelerations in first level, (**b**) accelerations in top level, (**c**) displacements in frame.

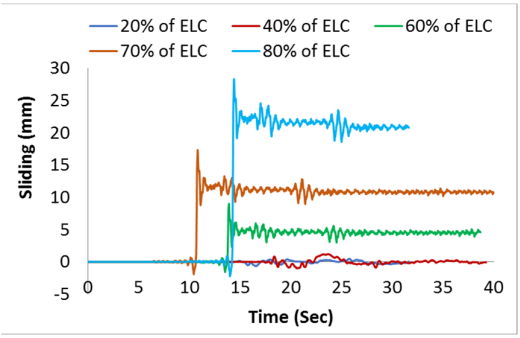

Figure 12. Pallet sliding of rack specimens—Non-Scaled in the time-domain.

Table 3. Peak responses of rack structure under seismic actions—Non-Scaled in time domain.

Intensity (% ELC)	Top Level Disp. (mm)	1st Level Disp. (mm)	Top Level Acc. (a/g)	1st Level Acc. (a/g)	Top Level Pallet Acc. (a/g)	1st Level Pallet Acc. (a/g)
20	16.4	10.0	0.15	0.086	0.15	0.083
40	47.5	39.1	0.31	0.23	0.33	0.23
60	60.6	47.7	0.52	0.29	0.5	0.285
70	68.4	52.6	0.61	0.35	0.54	0.327
80	76.2	58	0.69	0.425	0.545	0.396

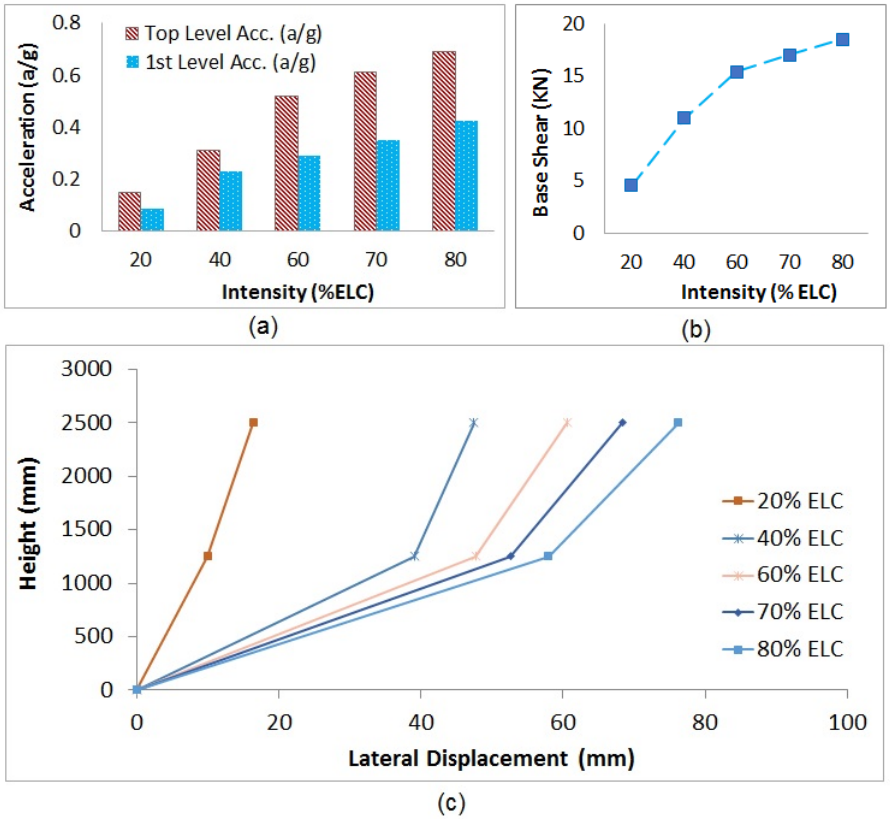

Figure 13. Comparison of rack results—Non-Scaled in the time domain: (**a**) frame acceleration, (**b**) frame base shear, (**c**) frame lateral displacement.

3.3. Results of Phase Three: Shake Table Tests (Scaled Down in Time Domain)

As the test specimen was limited to 3 meters height, the results may not be extendable for taller racks with a period longer than 0.63 s of the tested specimen. For this reason, to estimate the behaviour of taller rack frames under the same seismic actions, a similar rack configuration was subjected to the same El-Centro earthquake record, but scaled down in the time domain by a factor of 2. By using this technique, instead of changing the structure to obtain a more extended period (two times longer), the same structure was subjected to a faster earthquake. Therefore, the behaviour of a system with a given natural frequency under a squeezed time history record (e.g., faster earthquake) simulates the behaviour of a virtual structure with the longer period under a non-scaled earthquake in the time domain.

Figure 14 shows the structural responses for the ground motions with 40% to 220% intensities of El-Centro earthquake records with 20% increments in the scale time-domain condition. As shown, increasing the excitation intensity typically resulted in an increase in the acceleration of the system and the lateral displacement of the rack. In addition, from the test data, it was found that the front frame responses were almost identical to the back-frame results for all specimens. This indicates that the frames tended to deform as rigid bodies at each level with equal deformations at either side. As shown in Figure 15, pallets started to significantly slide on the beam after 160% intensity tests. This can be explained by the reduction in the friction coefficient between the timber pallet and the beam due to the large number of tests using the same pallets and beams, which smoothed the contact surfaces of the timber pallet with the beam flange. The tests were continued until the automatic acceleration sensor raised an alarm of reaching a high acceleration at the top level close to the table capacity during the 220% intensity test. The peak responses of the rack structure under the scaled time domain are given in Table 4.

Figure 16 shows the displacement time history measured at the top and first level of the rack starting from 40% intensity to 220% intensity of the El-Centro earthquake. Despite the large inelastic deformations in the down-aisle direction, the racks could still provide stability without compromising their vertical load-carrying capacity. The structure's lateral displacement again showed higher inter-storey drifts at the first level, as illustrated in Figure 16. The primary reason for higher drifts at the first level is attributed to the loss of stiffness at upright and beam connections below the first level, where the plastic hinges were formed and consequently led to a soft storey response. Figure 17 indicates the failure of the specimen at the upright to beam connection, which can be attributed to the soft storey mechanism. At the end of the test with 220% intensity, local failures were visible in the uprights along the first and second level.

The absolute peak acceleration of each level and the base shear for each seismic intensity are also shown in Figure 16. It is seen that the peak acceleration and base shear do not vary linearly with increasing the intensity of the earthquake. The peak acceleration recorded for specimens with a non-scaled time domain was between 0.15 and 0.7, while the corresponding peak acceleration for specimens under a scaled time domain was within a range of 0.1–0.5. In terms of peak lateral displacement, the peak displacements of specimens with a non-scaled time domain were between 15 mm and 78 mm, while for specimens with a scaled time domain the corresponding values were between 8 mm and 40 mm. By comparing the results of Figure 13 and Figure 16, it can be seen that decreasing the time domain by a factor of 2 resulted in lower acceleration magnitudes and, consequently, lower rack displacements and base shear values. This is due to the fact that taller rack systems with a longer period of vibration attract less seismic forces.

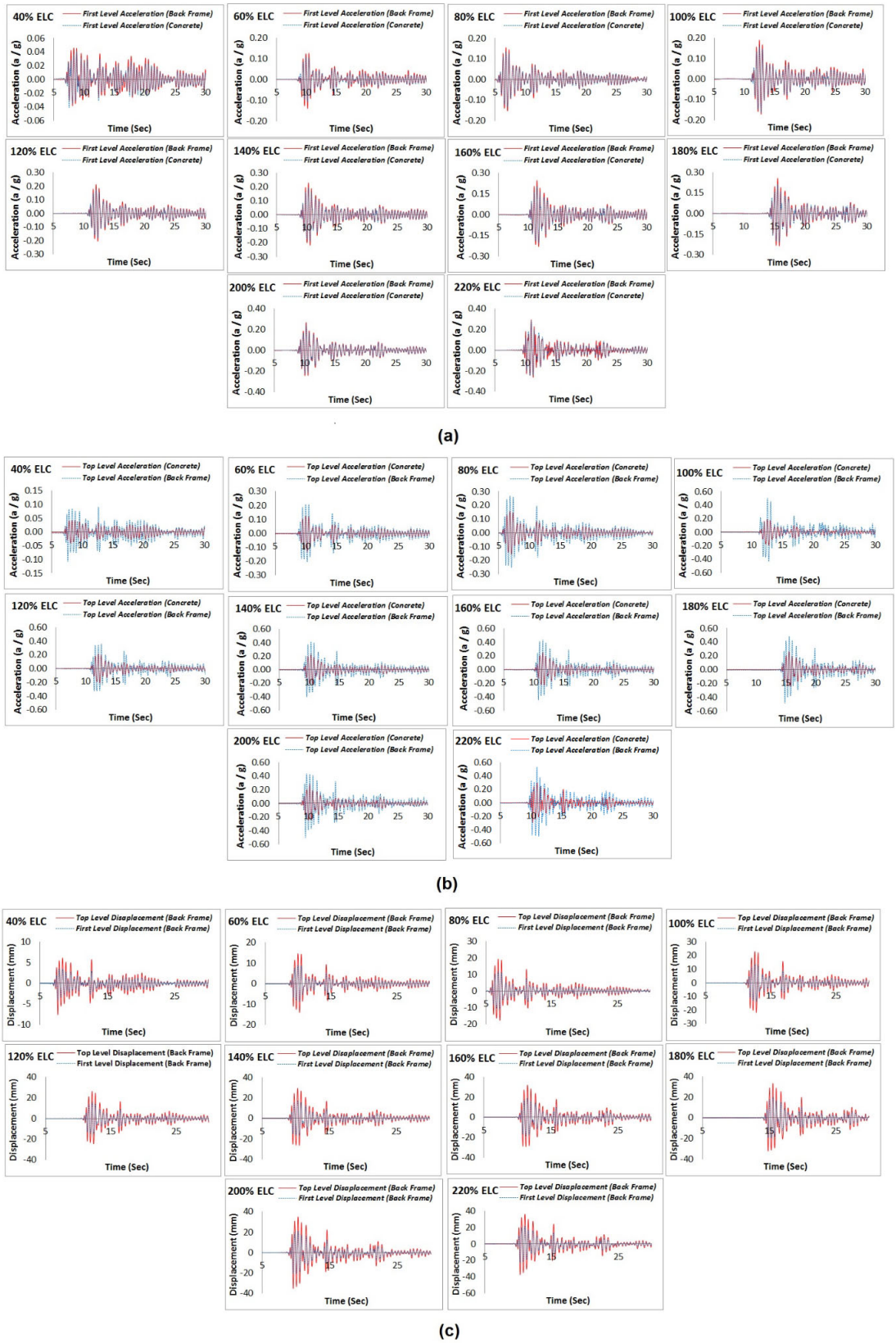

Figure 14. Structural response under 40–220% intensity of El-Centro earthquake record—Scaled down in time domain: (**a**) accelerations in first level, (**b**) accelerations in top level, (**c**) displacements in frame.

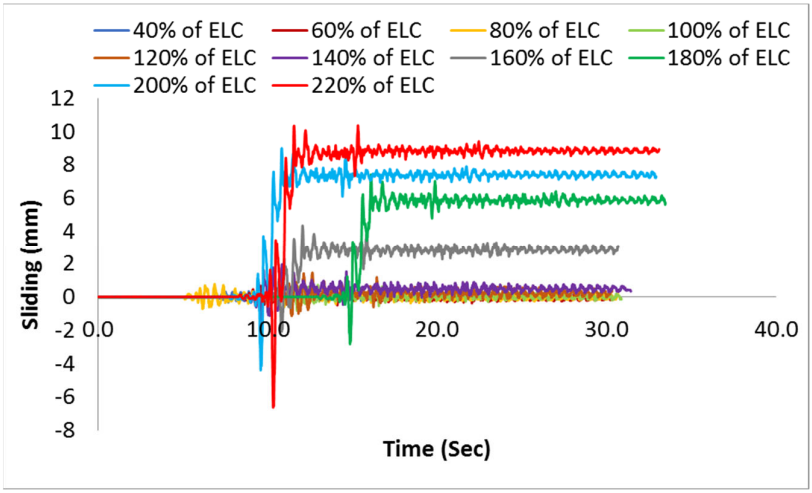

Figure 15. Pallet sliding of rack specimens—Scaled down in time domain.

Table 4. Peak responses of rack structure under seismic actions—Scaled down in time domain.

Intensity (% ELC)	Top Level Disp. (mm)	1st Level Disp. (mm)	Top Level Acc. (a/g)	1st Level Acc. (a/g)	Top Level Pallet Acc. (a/g)	1st Level Pallet Acc. (a/g)
40	9.21	5.76	0.132	0.08	0.078	0.068
60	14.56	8.95	0.21	0.14	0.13	0.11
80	19.31	11.84	0.27	0.16	0.16	0.14
100	22.94	13.81	0.33	0.19	0.19	0.16
120	26.36	15.70	0.36	0.21	0.22	0.18
140	29.43	17.45	0.42	0.23	0.23	0.19
160	31.85	19.05	0.45	0.25	0.25	0.21
180	33.42	20.20	0.48	0.26	0.26	0.22
200	35.39	21.19	0.50	0.27	0.28	0.23
220	37.82	22.91	0.52	0.28	0.29	0.24

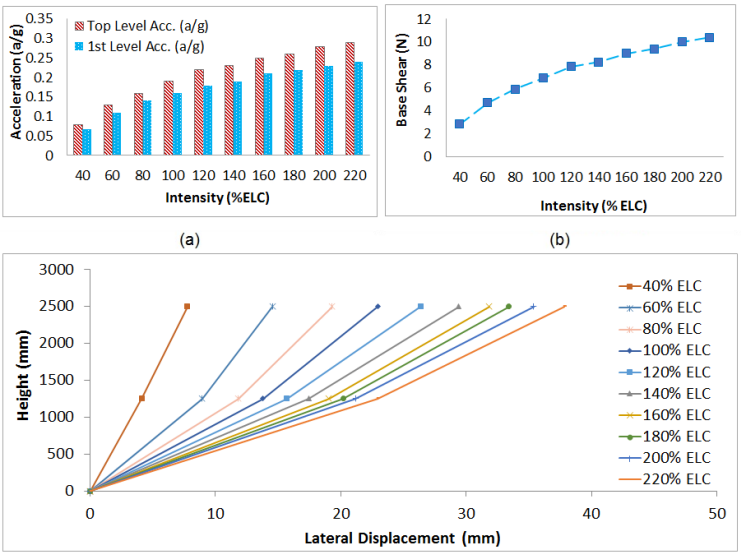

Figure 16. Comparison of rack results—Scaled down in time domain: (**a**) frame acceleration, (**b**) frame base shear, (**c**) frame lateral displacement.

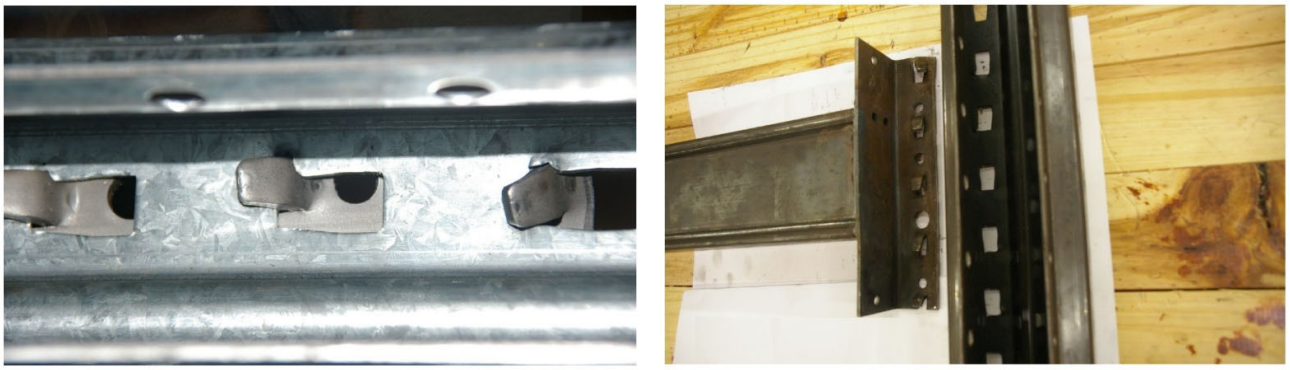

Figure 17. Failure at beam to upright connection.

4. Damping of the System

Another important dynamic characteristic is the structure's damping, which could be a significant source of energy dissipation. The damping of rack structures attributes to the dissipated energy of the rack components due to yielding and deformations as well as the friction in connections and the sliding of the pallets. However, it is hardly possible to identify or mathematically describe each of these energy dissipation mechanisms in an actual building [46]. Limited investigations on the damping of rack structures have been reported so far from previous shake table tests. Previous studies emphasized that the effect of the amplitude of motion on the damping ratio is significant, and the structural damping is affected by the looseness of the connections. However, a damping ratio for the seismic design of rack structures has not yet been proposed with a high level of confidence. However, proposing a precise damping ratio is beyond the scope of this study and indeed needs more in situ testing of loaded and unloaded racks.

The damping characteristic of structures and buildings is mathematically known as the damping ratio (ξ), which is the normalized damping coefficient of the structure with respect to its critical damping. The fundamental period of vibration, T, and its corresponding damping ratio are the main parameters to predict the behaviour of buildings and structures under given dynamic loads. One of the few practical ways to determine the fundamental period of a structure and the damping ratio related to that period is by obtaining the frequency-response curve experimentally. This task can be carried out by performing sinusoidal sweep testing (a forced vibration test) using sinusoidal (harmonic) loading over a range of frequencies. The concept is to excite the structure with harmonic loading such that at certain periods (periods of vibration, T_i) the structure experiences resonance. Damping ratios corresponding to each frequency of vibration can be determined by using the half power band method, as displayed in Figure 18.

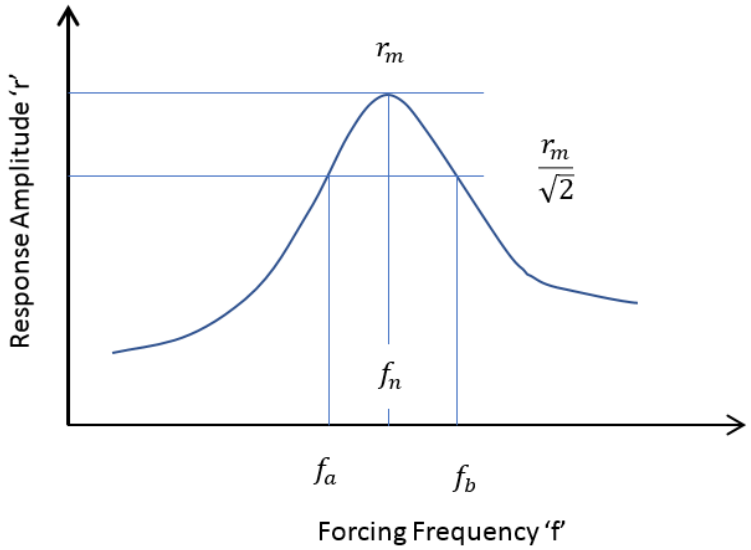

Figure 18. Evaluating damping from the frequency-response curve.[47]

Then, the damping ratio can be calculated by the equation below:

$$\xi(\%) = \frac{f_b - f_a}{2f_n} \quad (1)$$

where f_n is the forcing frequency at resonance and f_a and f_b are the calculated frequencies at a response amplitude of $1/\sqrt{2}$ of the peak response amplitude [47].

As mentioned earlier, after every step of the shake table tests, the structure was subjected to a sine sweep wave with an acceleration amplitude of "0.02g" in order to evaluate the damping ratio and vibration period elongations due to cumulative damage in the system. Table 5 shows the damping ratios as well as the fundamental vibration period of the system calculated from the sine sweep tests conducted after each of the test steps for both non-scaled and scaled time-domain conditions. Damping ratios were then calculated by applying the half-power band method on the sine sweep test results. The results of this table show an increase in the damping ratios after each increment of the shake table test with increasing seismic intensity. The corresponding increase in the amount of lateral movement of the frame is basically the result of the interactions of the hooks in the beam end connectors and upright slots. As the displacement amplitude in the scaled tests in the time domain was smaller than in the non-scaled tests, lower damping ratios were obtained for the former condition.

Figure 19 shows the frequency–response curves of the sine sweep test results used to obtain the damping ratio as well as the fundamental period of vibration. For the non-scaled tests, the period was visibly changed due to the apparent damage of the system in dissipative zones (e.g., connections), and the system lost stiffness. The increase in the damping ratio due to enhancing the intensity of the earthquake can also be seen in the graphs by focusing on the width of the curves that were broadened.

Table 5. Dynamic features of the system under 1940 El-Centro test record.

Time-Domain Scale	Intensity (%ELC)	Frequency (Hz)	Damping Ratio (%)	Top Level Displacement (mm)
Non scaled	60	1.5	16.7	60.4
	70	1.4	18.6	68.4
	80	1.35	19.2	76.2
Scaled	Before Tests	1.85	5.3	0
	40	1.85	6.8	9.21
	60	1.85	6.8	14.56
	80	1.85	7.4	19.31
	100	1.85	7.4	22.94
	120	1.85	7.5	26.36
	140	1.80	7.7	29.43
	160	1.80	7.3	31.85
	180	1.75	7.7	33.42
	200	1.70	8.1	35.39
	220	1.65	8.0	37.82

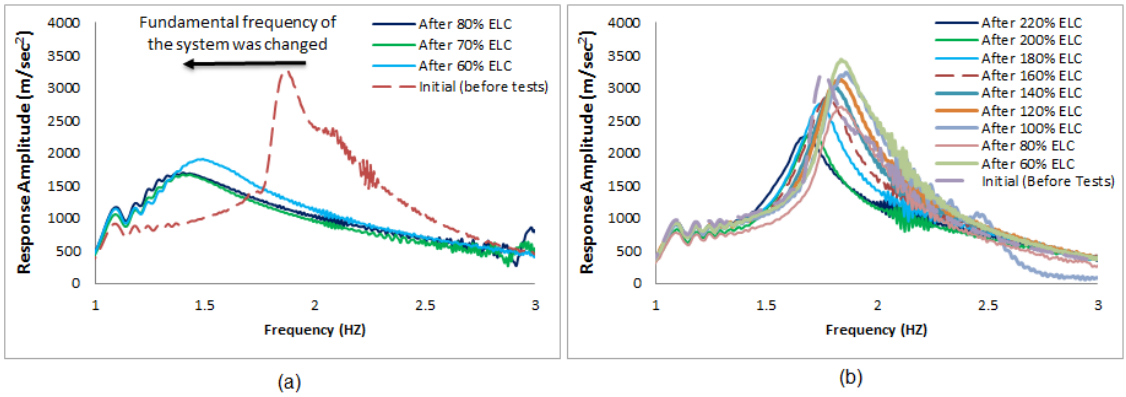

Figure 19. Sine sweep test results: (**a**) non-scaled test in time domain, (**b**) scaled test in time domain.

However, unlike damping ratios, the fundamental period of the structure has not been significantly shifted after higher seismic records. Nevertheless, both the effects of "sharp damping increase" and "negligible vibration period change" cannot be extrapolated to the overall nonlinear behaviour of every rack structure. This is because all these results are derived from sine sweep tests with a very low acceleration intensity of "0.02 g" during small displacements, and hence the system behaves elastically. On the other hand, increasing the acceleration intensity is unsafe and impractical due to the uncertainties of the system at resonance. The damping ratios determined from structural motions that are small are not representative of the larger damping expected at higher amplitudes of structural motion [47].

Under such low-intensity sine sweep tests, the hooks mainly slide in the slots, which cause high damping ratios due to the hook-to-slot friction. After running high-intensity seismic records in which the structure experiences greater lateral movement, the hooks in the connection area cut into the upright slots and create a higher travel pass for the next hook-slot interactions. This may explain why the damping ratios calculated from the sine sweep tests performed after high seismic shake table tests are drastically higher. The above explanation can be supported by the phenomenon of making loud noises while running sine sweep tests. The noise was possibly because of sliding and the relative movement between the hook and the upright slot. However, the system still showed more

damping after it was subjected to higher seismic intensities, or in general, when the system is no longer linear, it shows more damping.

5. Conclusion and Recommendations

Details of the experimental results of shake table tests on standard storage racks in the down-aisle direction were presented in this paper. To generate data on the seismic inelastic response of a standard rack system in New Zealand, a 2 level—2 bay frame was subjected to El-Centro earthquake records with different intensities in an increasing fashion from low to high intensities. The test results were measured and the data were analysed in terms of natural frequency, rack frame deformations and accelerations, pallet sliding and accelerations as well as the damping of the system. Shake table test results proved that the inter-storey drift at the first level of the structure was greater than that of the second level (soft storey mechanism), and this effect became more obvious at higher intensity earthquakes. This effect could have been justified by the low stiffness of connections, which needs to be considered for the design of rack structures. Pallet sliding was also observed during all seismic tests. The test proved that the pallet slid significantly on top of the beams, but the movement was not that much to push the pallet off the beam. The difference between the recorded acceleration data from the accelerometers mounted on the beams and the data from accelerometers mounted at the concrete blocks (on the pallets) highlighted the effect of sliding in reducing the seismic base shear for seismic design. It was observed that the rack lateral displacement, base shear and accelerations, as well as pallet sliding under actual time-domain conditions, are higher than when the time domain is scaled down (owing to shrunk ground motion acceleration history). The damping ratio of the system at each step was also calculated, and an increasing trend in the damping ratio versus the maximum lateral displacement of the systems was discovered. However, much higher damping values are expected for larger response amplitudes caused by strong ground motion excitations.

It should be noted that the specimens in this study were defined based on New Zealand standard storage rack pallets. Therefore, the discussion provided in this study is specific for this presented configuration. Although the results may be applied to other similar racks, each rack frame has its own characteristics, some of which can significantly change the results under the seismic loading.

The experimental data of this study can be utilized for developing numerical simulations [48] or numerical algorisms [49] to perform a parametric study on storage rack frames and evaluate the dynamic behaviour of rack frames under different conditions. The effects of loading in the transverse direction must also be considered in future studies.

Author Contributions: Conceptualization, A.F. and B.S.; methodology, A.F. and N.U.; formal analysis, A.F. and N.U.; investigation, A.F.; resources, A.F.; writing—original draft preparation, A.F. and N.U.; writing—review and editing, A.F., N.U. and P.M.; visualization, N.U. and P.M.; supervision, B.S.; project administration, B.S. All authors have read and agreed to the published version of the manuscript.

Institutional Review Board Statement: Not applicable.

Informed Consent Statement: Not applicable.

Acknowledgments: The authors would like to acknowledge the contribution by Dexion Australia for providing the materials of rack frames and Ali Saleh in supporting this study.

Conflicts of Interest: The authors declare no conflict of interest.

References

1. Ng, A.L.Y.; Beale, R.G.; Godley, M.H.R. Methods of restraining progressive collapse in rack structures. *Eng. Struct.* **2009**, *31*, 1460–1468, doi:10.1016/j.engstruct.2009.02.029.
2. Javidan, M.M.; Kang, H.; Isobe, D.; Kim, J. Computationally efficient framework for probabilistic collapse analysis of structures under extreme actions. *Eng. Struct.* **2018**, *172*, 440–452.
3. Mohajeri Nav, F.; Usefi, N.; Abbasnia, R. Analytical investigation of reinforced concrete frames under middle column removal scenario. *Adv. Struct. Eng.* **2018**, *21*, 1388–1401, doi:10.1177/1369433217746343.
4. Ahmadi, R.; Rashidian, O.; Abbasnia, R.; Mohajeri Nav, F.; Usefi, N. Experimental and numerical evaluation of progressive collapse behavior in scaled RC beam-column subassemblage. *Shock Vib.* **2016**, *2016*, 3748435.
5. Shayanfar, M.A.; Javidan, M.M. Progressive collapse-resisting mechanisms and robustness of RC frame–shear wall structures. *J. Perform. Constr. Facil.* **2017**, *31*, 04017045.
6. RMI. *Specification for the Design, Testing and Utilization of Industrial Steel Storage Racks*; RMI: Basalt, CO, USA, 1997
7. *Steel Static Storage Systems—Adjustable Pallet Racking Systems—Principles for Structural Design, EN 16681*; European Committee for Standardization: Brussels, Belgium, 2016.
8. Liu, P.; Peterman, K.; Schafer, B. *Test Report on Cold-Formed Steel Shear Walls*; Johns Hopkins University: Baltimore, MD, USA 2012.
9. *Seismic Considerations for Steel Storage Racks Located in Areas Accessible to the Public, FEMA460*; Federal Emergency Management Agency: Washington, DC, USA, 2005.
10. *User Guide for Steel Storage Racks, CSA A344*; Canadian Standards Association: Toronto, ON, Canada, 2017.
11. *Specification For The Design, Testing And Utilization Of Industrial Steel Storage Racks, ANSI MH16*; Rack Manufacturer's Institute: Charlotte, CA, USA, 2012.
12. Vassiliou, M.F.; Mackie, K.R.; Stojadinović, B. A finite element model for seismic response analysis of deformable rocking frames. *Earthq. Eng. Struct. Dyn.* **2017**, *46*, 447–466.
13. Di Egidio, A.; Alaggio, R.; Aloisio, A.; de Leo, A.M.; Contento, A.; Tursini, M. Analytical and experimental investigation into the effectiveness of a pendulum dynamic absorber to protect rigid blocks from overturning. *Int. J. Non-Linear Mech.* **2019**, *115*, 1–10.
14. Elias, G.C.; de Almeida Neiva, L.H.; Sarmanho, A.M.C.; Alves, V.N.; Castro, A.F.B.E. Ultimate load of steel storage systems uprights. *Eng. Struct.* **2018**, *170*, 53–62.
15. Yin, L.; Tang, G.; Zhang, M.; Wang, B.; Feng, B. Monotonic and cyclic response of speed-lock connections with bolts in storage racks. *Eng. Struct.* **2016**, *116*, 40–55.
16. Taheri, E.; Firouzianhaji, A.; Usefi, N.; Mehrabi, P.; Ronagh, H.; Samali, B. Investigation of a Method for Strengthening Perforated Cold-Formed Steel Profiles under Compression Loads. *Appl. Sci.* **2019**, *9*, 5085.
17. Taheri, E.; Firouzianhaji, A.; Mehrabi, P.; Hosseini, B.V.; Samali, B. Experimental and Numerical Investigation of a Method for Strengthening Cold-Formed Steel Profiles in Bending. *Appl. Sci.* **2020**, *10*, 3855.
18. Kanyilmaz, A.; Castiglioni, C.A.; Brambilla, G.; Chiarelli, G.P. Experimental assessment of the seismic behavior of unbraced steel storage pallet racks. *Thin-Walled Struct.* **2016**, *108*, 391–405.
19. Bernuzzi, C.; Di Gioia, A.; Gabbianelli, G.; Simoncelli, M. Pushover analyses of hand-loaded steel storage shelving racks. *J. Earthq. Eng.* **2017**, *21*, 1256–1282.
20. Adamakos, K.; Vayas, I.; Avgerinou, S. Estimation of the behavior factor of steel storage pallet racks. In Proceedings of the 4th ECCOMAS Thematic Conference on Computational Methods in Structural Dynamics and Earthquake Engineering, Kos Island, Greece, 12–14 June 2013.
21. Campiche, A. Numerical Modelling of CFS Three-Story Strap-Braced Building under Shaking-Table Excitations. *Materials* **2021**, *14*, 118.
22. Chen, C.; Scholl, R.; Blume, J. Earthquake simulation tests of industrial steel storage racks. In Proceedings of the Seventh World Conference on Earthquake Engineering, Istanbul, Turkey, 8–13 September 1980; pp. 379–386.
23. Chen, C.; Scholl, R.; Blume, J. *Seismic Study of Industrial Storage Racks, Report Prepared for the National Science Foundation for the Rack Manufacturers Institute Automated Storage Retrieval Systems*; URS/John A. Blume & Associates: San Francisco, CA, USA, 1980.
24. Chen, C.; Blume, J.A.; Scholl, R.E. Seismic-Resistant Design of Industrail Storage Racks. In Proceedings of the Dynamic Response of Structures: Experimentation, Observation, Prediction and Control, Atlanta, GA, USA, 15–16 December 1981; pp. 745–759.
25. Filiatrault, A.; Higgins, P.S.; Wanitkorkul, A. Experimental stiffness and seismic response of pallet-type steel storage rack connectors. *Pract. Period. Struct. Des. Constr.* **2006**, *11*, 161–170.
26. Filiatrault, A.; Wanitkorkul, A. *Shake-Table Testing of Frazier Industrial Storage Racks*; Report No. CSEE-SEESL-2005-02; Structural Engineering and Earthquake, University at Buffalo: Buffalob, NY, USA, 2004.
27. Sideris, P.; Filiatrault, A.; Leclerc, M.; Tremblay, R. Experimental investigation on the seismic behavior of palletized merchandise in steel storage racks. *Earthq. Spectra* **2010**, *26*, 209–233.
28. Simoncelli, M.; Tagliafierro, B.; Montuori, R. Recent development on the seismic devices for steel storage structures. *Thin-Walled Struct.* **2020**, *155*, 106827.
29. Mohammadi, M.; Kafi, M.A.; Kheyroddin, A.; Ronagh, H. Performance of innovative composite buckling-restrained fuse for concentrically braced frames under cyclic loading. *Steel Compos. Struct. Int. J.* **2020**, *36*, 163–177.

30. Mohammadi, M.; Kafi, M.A.; Kheyroddin, A.; Ronagh, H.R. Experimental and numerical investigation of an innovative buckling-restrained fuse under cyclic loading. *Structures* **2019**, *22*, 186–199.
31. Sharafi, P.; Mortazavi, M.; Usefi, N.; Kildashti, K.; Ronagh, H.; Samali, B. Lateral force resisting systems in lightweight steel frames: Recent research advances. *Thin-Walled Struct.* **2018**, *130*, 231–253.
32. Azandariani, M.G.; Rousta, A.M.; Usefvand, E.; Abdolmaleki, H.; Azandariani, A.G. Improved seismic behavior and performance of energy-absorbing systems constructed with steel rings. *Structures* **2021**, *29*, 534–548.
33. Azandariani, M.G.; Azandariani, A.G.; Abdolmaleki, H. Cyclic behavior of an energy dissipation system with steel dual-ring dampers (SDRDs). *J. Constr. Steel Res.* **2020**, *172*, 106145.
34. Rosin, I.; Proenca, J; Calado, L; Carydis, P.; Mouzakis, H.; Castiglioni, C.; Brescianini, J.C.; Plumier, A.; Degee, H.; Negro, P; Molina, F. *Storage Racks in Seismic Areas, EUR 23744EN*; European Commision: Luxembourg, 2009.
35. Gilbert, B.P.; Rasmussen, K.J. Drive-in steel storage racks I: Stiffness tests and 3D load-transfer mechanisms. *J. Struct. Eng.* **2012**, *138*, 135–147.
36. Shaheen, M.S.; Rasmussen, K.J. Seismic tests of drive-in steel storage racks in cross-aisle direction. *J. Constr. Steel Res.* **2019**, *162*, 105701.
37. Maguire, J.R.; Teh, L.H.; Clifton, G.C.; Tang, Z.; Lim, J.B. Cross-aisle seismic performance of selective storage racks. *J. Constr. Steel Res.* **2020**, *168*, 105999.
38. Baldassino, N.; Bernuzzi, C.; di Gioia, A.; Simoncelli, M. An experimental investigation on solid and perforated steel storage racks uprights. *J. Constr. Steel Res.* **2019**, *155*, 409–425.
39. Rainieri, C.; Fabbrocino, G. *Operational Modal Analysis of Civil Engineering Structures*; Springer: Berlin/Heidelberg, Germany, 2014; Volume 142, p. 143.
40. Aloisio, A.; Di Pasquale, A.; Alaggio, R.; Fragiacomo, M. Assessment of seismic retrofitting interventions of a masonry palace using operational modal analysis. *Int. J. Archit. Herit.* **2020**, 1–13, doi:10.1080/15583058.2020.1836531.
41. Jacobsen, E.; Tremblay, R. Shake-table testing and numerical modelling of inelastic seismic response of semi-rigid cold-formed rack moment frames. *Thin-Walled Struct.* **2017**, *119*, 190–210.
42. Krawinkler, H. *Experimental Study on Seismic Behavior of Industrial Storage Racks*; Blume Earthquake Engineering Center: Stanford, CA, USA, 1978. Availabe online: https://core.ac.uk/download/pdf/229100879.pdf (accessed on 17 February 2021)
43. Javidan, M.M.; Kim, J. Seismic Retrofit of Soft-First-Story Structures Using Rotational Friction Dampers. *J. Struct. Eng.* **2019**, *145*, 04019162, doi:10.1061/(ASCE)ST.1943-541X.0002433.
44. Javidan, M.M.; Kim, J. Steel hysteretic column dampers for seismic retrofit of soft-first-story structures. *Steel Compos. Struct.* **2020**, *37*, 259–272.
45. Javidan, M.M.; Kim, J. Variance—Based global sensitivity analysis for fuzzy random structural systems. *Comput.-Aided Civ. Infrastruct. Eng.* **2019**, *34*, 602–615.
46. Carneiro, J.; Demelo, F.; Jalali, S.; Teixeira, V.; Tomas, M. The use of pseudo-dynamic method in the evaluation of damping characteristics in reinforced concrete beams having variable bending stiffness. *Mech. Res. Commun.* **2006**, *33*, 601–613.
47. Chopra, A.K. *Dynamics of Structures Theory and Applications to Earthquake Engineering*; Prentice—Hall, Englewood Cliffs: Upper Saddle River, NJ, USA, 1995.
48. Usefi, N.; Sharafi, P.; Ronagh, H. Numerical models for lateral behaviour analysis of cold-formed steel framed walls: State of the art, evaluation and challenges. *Thin-Walled Struct.* **2019**, *138*, 252–285.
49. Mehrabi, P.; Honarbari, S.; Rafiei, S.; Jahandari, S.; Bidgoli, M.A. Seismic response prediction of FRC rectangular columns using intelligent fuzzy-based hybrid metaheuristic techniques. *J. Ambient. Intell. Humaniz. Comput.* **2021**, 1–19, doi:10.1007/s12652-020-02776-4.